Ram, S., Abraham, A., Ward, E. S., and Ober, R. J. A novel 3D resolution measure for optical microscopes with applications to single molecule imaging. *Ultrasensitive and Single-Molecule Detection Technologies II. SPIE International Symposium on Biomedical Optics (BiOS)*, 6444: 6440-D9, 2007.

A novel 3D resolution measure for optical microscopes with applications to single molecule imaging

Sripad Ram[a,b], Anish V. Abraham[a,c], E. Sally Ward[a] and Raimund J. Ober[a,d]

[a]Center for Immunology, University of Texas Southwestern Medical Center, Dallas, TX, USA;
[b]Joint Biomedical Engineering Graduate Program, University of Texas at Arlington/University of Texas Southwestern Medical Center, Dallas, TX, USA;
[c]Department of Computer Science, University of Texas at Dallas, Richardson, TX, USA,
[d]Department of Electrical Engineering, University of Texas at Dallas, Richardson, TX, USA.

ABSTRACT

The advent of single molecule microscopy has generated significant interest in imaging single biomolecular interactions within a cellular environment in three dimensions. It is widely believed that the classical 2D (3D) resolution limit of optical microscopes precludes the study of single molecular interactions at distances of less than 200 nm (1 micron). However, it is well known that the classical resolution limit is based on heuristic notions. In fact, recent single molecule experiments have shown that the 2D resolution limit, i.e. Rayleigh's criterion, can be surpassed in an optical microscope setup. This illustrates that Rayleigh's criterion is inadequate for modern imaging approaches, thereby necessitating a re-assessment of the resolution limits of optical microscopes. Recently, we proposed a new modern resolution measure that overcomes the limitations of Rayleigh's criterion. Known as the fundamental resolution measure FREM, the new result predicts that distances well below the classical 2D resolution limit can be resolved in an optical microscope. By imaging closely spaced single molecules, it was experimentally verified that the new resolution measure can be attained in an optical microscope setup. In the present work, we extend this result to the 3D case and propose a 3D fundamental resolution measure 3D FREM that overcomes the limitations of the classical 3D resolution limit. We obtain an analytical expression for the 3D FREM. We show how the photon count of the single molecules affects the 3D FREM. We also investigate the effect of deteriorating experimental factors such as pixelation of the detector and extraneous noise sources on the new resolution measure. In contrast to the classical 3D resolution criteria, our new result predicts that distances well below the classical limit can be resolved. We expect that our results would provide novel tools for the design and analysis of 3D single molecule imaging experiments.

Keywords: 3D resolution criterion, Rayleigh's criterion, Fisher information matrix, Cramer-Rao lower bound

1. INTRODUCTION

In the recent past, advances in detector technology and fluorescent labeling methodology including green fluorescent protein based methods have made it possible to detect single molecules even in a cellular environment (e.g., see Ref. 1). The study of single biomolecular interactions, such as protein-protein interactions, is important for understanding cellular processes. These interactions typically take place at nanometer scale distances. However, it has long been thought that such interactions cannot be imaged with a regular optical microscope due to the limitations imposed by the classical resolution criteria. For instance, it is widely believed that Rayleigh's criterion precludes the study of single molecular interactions at distances of less than 200 nm in the plane of focus. Despite this, it is well known that Rayleigh's criterion is based on heuristic notions. Formulated within a deterministic framework, Rayleigh's criterion neglects the stochastic nature of the acquired data and therefore it does not take into account the total number of detected photons. Hence Rayleigh's criterion is not well adapted to current microscope setups that use highly sensitive photon counting cameras. Not surprisingly, recent single molecule experiments have shown that Rayleigh's criterion can in fact be surpassed in an optical microscope.[2–5] Thus, Rayleigh's criterion is inadequate for modern quantitative imaging techniques.

Classically, Rayleigh's criterion has been used as a tool to evaluate the feasibility of carrying out experiments that involve distance determination between two identical point sources. However, the inadequacy of Rayleigh's criterion, especially in the context of single molecule microscopy, suggests the need for a new resolution measure that is adapted to modern imaging approaches. In particular, for proper planning of an experiment, it is important to have a methodology available to be able to assess with what accuracy the distance between two single molecules can be determined. Recently, we proposed a new resolution measure[5] FREM (fundamental resolution measure) that overcomes the shortcomings of Rayleigh's criterion and provides a quantitative measure of the microscope's ability to determine the distance between two point sources. The FREM, unlike Rayleigh's criterion, predicts that the resolution of a microscope can be improved by increasing the number of photons collected from the point sources. Results were also presented that took into account the effect of pixelation and noise sources. By estimating distances from images of closely spaced single molecules, it was verified that distances well below Rayleigh's resolution limit can be determined with an accuracy as specified by the new resolution measure.[5]

Rayleigh's resolution criterion was formulated for the scenario when both point sources are in focus with respect to the objective lens. However, in many practical situations the point sources need not lie in the plane of focus and, in general, can be at any arbitrary location in 3D space. In such cases, it is important to know the 3D resolvability of single molecules. In the present work, we extend our previous result to the three-dimensional case and propose a 3D fundamental resolution measure 3D FREM. We derive an analytical formula for the 3D FREM. Analogous to our previous result,[5] we show that the new 3D resolution measure depends on the photon statistics of the acquired data. In particular we show that the 3D resolvability of single molecules can be improved by increasing the number of detected photons from the single molecules. We also investigate the effect of deteriorating experimental factors such as pixelation of the detector and the presence of extraneous noise sources.

2. GENERAL STOCHASTIC FRAMEWORK

The underlying approach to the derivation of the new resolution measure is given elsewhere.[5,6] Here we provide a brief description in the context of the 3D resolution problem. The data acquired in a fluorescence microscope setup is stochastic in nature, since the photon emission process is intrinsically a random phenomenon. Here we consider experiments in which the data is acquired for a fixed time interval. We formulate the task of determining the distance between two point sources as a parameter estimation problem. The distance of separation is obtained by using an unbiased estimation procedure, and the performance of this estimator is given by the standard deviation of the distance estimates assuming repeated experiments. According to the Cramer-Rao inequality,[7] the (co)variance of any unbiased estimator $\hat{\theta}$ of an unknown parameter θ is always greater than or equal to the inverse Fisher information matrix, i.e.,

$$\text{Cov}(\hat{\theta}) \geq \mathbf{I}^{-1}(\theta).$$

An important property of the Fisher information matrix is that it is independent of how the parameter is estimated and only depends on the statistical description of the acquired data. Because the performance of an unbiased estimator is given by its standard deviation, the above inequality implies that the square root (of the corresponding leading diagonal entry) of the inverse Fisher information matrix provides a lower bound to the performance of any unbiased estimator of θ. Hence we define the 3D resolution measure as the square root (of the corresponding leading diagonal entry) of the inverse Fisher information matrix that corresponds to the distance estimation problem between two point sources.

2.1. Fisher information matrix

For a general parameter estimation problem in optical microscopy, the expression for the Fisher information matrix corresponding to the acquisition time interval $[t_0, t]$ is given by[6,8]

$$\mathbf{I}(\theta) := \int_{t_0}^{t} \int_{\mathcal{C}} \frac{1}{\Lambda_\theta(\tau) f_{\theta,\tau}(r)} \left(\frac{\partial [\Lambda_\theta(\tau) f_{\theta,\tau}(r)]}{\partial \theta} \right)^T \frac{\partial [\Lambda_\theta(\tau) f_{\theta,\tau}(r)]}{\partial \theta} dr d\tau, \quad \theta \in \Theta. \tag{1}$$

The acquired data is modeled as a spatio-temporal random process, which we refer to as the image detection process. A detailed discussion of this process is given elsewhere,[5] and here we provide a brief description. The

temporal part is an inhomogeneous Poisson process with intensity function Λ_θ, and models the time points of the detected photons. The spatial part consists of a sequence of independent random variables with densities $\{f_{\theta,\tau}\}_{\tau \geq t_0}$ and models the spatial coordinates of the detected photons. In the above expression, $\mathcal{C} \subseteq \mathbb{R}^2$ denotes the detector that is used to collect the photons. It is assumed that the spatial and the temporal components are mutually independent of each other. In deriving eq. 1 no specific assumptions have been made regarding the functional form of Λ_θ or $f_{\theta,\tau}$. Therefore, the above expression of $\mathbf{I}(\theta)$ is applicable to a wide variety of imaging conditions, such as coherent and incoherent illumination. We note that an implication of the time dependence of the density function $f_{\theta,\tau}$ is that the above expression of $\mathbf{I}(\theta)$ is also applicable to moving objects.
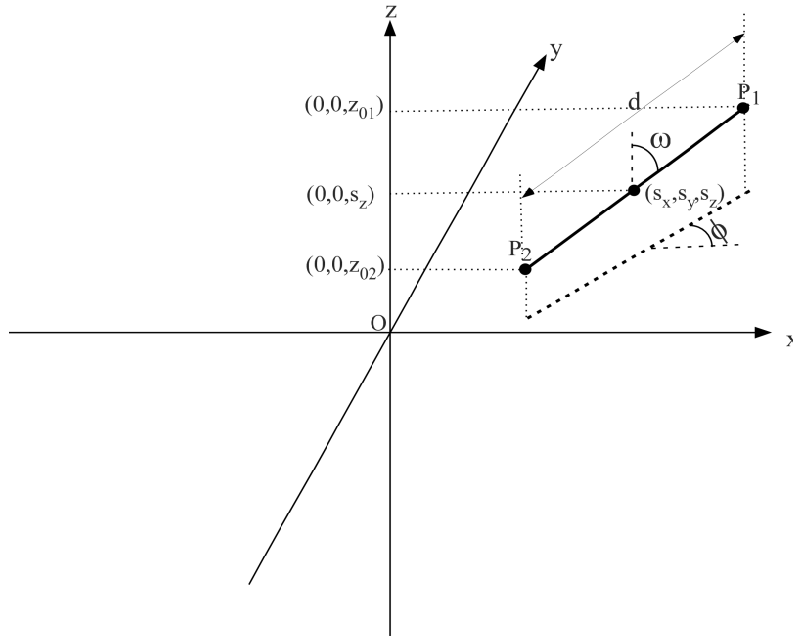
Figure 1. Schematic illustrating the notation used to specify the 3D location of two single molecules P_1 and P_2.

In single molecule data analysis, the photon detection rate of the single molecule can be determined apriori from calibration experiments and therefore can be assumed to be known when estimating the desired attribute(s) from the data. Hence the intensity function is given by $\Lambda_\theta(\tau) = \Lambda_1(\tau) + \Lambda_2(\tau)$, $\tau \geq t_0$, where Λ_1 and Λ_2 denote the photon detection rates of the two single molecules. The unknown parameter vector is given by $\theta = d \in \Theta$, where d denotes the distance of separation between the two single molecules and $\Theta \subseteq [0,\infty)$ denotes the parameter space. For the 3D resolution problem, the density function $f_{\theta,\tau}$ can be written as (see Fig. 1)

$$f_{\theta,\tau}(r) := \frac{\epsilon_1(\tau)}{M^2} q_{z_{01}(d),1} \left(\frac{x}{M} - s_x - \frac{d \sin \omega}{2} \cos \phi, \frac{y}{M} - s_y - \frac{d \sin \omega}{2} \sin \phi \right)$$

$$+ \frac{\epsilon_2(\tau)}{M^2} q_{z_{02}(d),2} \left(\frac{x}{M} - s_x + \frac{d \sin \omega}{2} \cos \phi, \frac{y}{M} - s_y + \frac{d \sin \omega}{2} \sin \phi \right), \tag{2}$$

where $r = (x,y) \in \mathbb{R}^2$, $\theta \in \Theta$, and $\tau \geq t_0$. In the above equation, $\epsilon_i(\tau) := \Lambda_i(\tau)/(\Lambda_1(\tau) + \Lambda_2(\tau))$, $i = 1,2$, $\tau \geq t_0$, d denotes the distance of separation between the two single molecules, ω and ϕ denote the orientation angles of the line joining the two single molecules as shown in Fig. 1, $z_{01}(d)$ and $z_{02}(d)$ denote the axial coordinates of the two single molecules, M denotes the magnification of the imaging system and $q_{z_{01}(d),1}$ and $q_{z_{02}(d),2}$ denote the image functions of the two single molecules. An image function q_{z_0} is defined as the image of an object at unit magnification when the object is located at $(0, 0, z_0)$, $z_0 \in \mathbb{R}$, in the object space. From fig. 1 we see that the axial coordinates z_{01} and z_{02} are functions of the distance d, since $z_{01}(d) := s_z + \frac{d}{2} \cos \omega$ and $z_{02}(d) := s_z - \frac{d}{2} \cos \omega$, where s_z denotes the axial coordinate of the midpoint of the line segment P_1P_2 (see Fig. 1). By definition, $f_{\theta,\tau}$

is assumed to satisfy the regularity conditions that are necessary for the calculation of the Fisher information matrix. Hence we impose appropriate conditions on the image function (see Ref. 6 for details).

Substituting for $f_{\theta,\tau}$ and Λ_θ in eq. 1 and simplifying, we obtain a general expression of the Fisher information matrix for the 3D resolution problem, which is given by[9]

$$
\mathbf{I}(\theta) = \frac{1}{4} \int_{t_0}^{t} \int_{\mathbb{R}^2} \frac{1}{\Lambda_1(\tau)q_{z_{01}(d),1}\left(x - \frac{d\sin\omega}{2}\cos\phi, y - \frac{d\sin\omega}{2}\sin\phi\right) + \Lambda_2(\tau)q_{z_{02}(d),2}\left(x + \frac{d\sin\omega}{2}\cos\phi, y + \frac{d\sin\omega}{2}\sin\phi\right)} \times
$$

$$
\left(\sin\omega\cos\phi \left[\Lambda_1(\tau) \frac{\partial q_{z_{01}(d),1}\left(x - \frac{d\sin\omega}{2}\cos\phi, y - \frac{d\sin\omega}{2}\sin\phi\right)}{\partial x} - \Lambda_2(\tau) \frac{\partial q_{z_{02}(d),2}\left(x + \frac{d\sin\omega}{2}\cos\phi, y + \frac{d\sin\omega}{2}\sin\phi\right)}{\partial x} \right] \right.
$$

$$
+ \sin\omega\sin\phi \left[\Lambda_1(\tau) \frac{\partial q_{z_{01}(d),1}\left(x - \frac{d\sin\omega}{2}\cos\phi, y - \frac{d\sin\omega}{2}\sin\phi\right)}{\partial y} - \Lambda_2(\tau) \frac{\partial q_{z_{02}(d),2}\left(x + \frac{d\sin\omega}{2}\cos\phi, y + \frac{d\sin\omega}{2}\sin\phi\right)}{\partial y} \right]
$$

$$
\left. - \cos\omega \left[\Lambda_1(\tau) \frac{\partial q_{z_{01}(d),1}\left(x - \frac{d\sin\omega}{2}\cos\phi, y - \frac{d\sin\omega}{2}\sin\phi\right)}{\partial z_{01}(d)} - \Lambda_2(\tau) \frac{\partial q_{z_{02}(d),2}\left(x + \frac{d\sin\omega}{2}\cos\phi, y + \frac{d\sin\omega}{2}\sin\phi\right)}{\partial z_{02}(d)} \right] \right)^2 dx\,dy\,d\tau,
$$

(3)

where $\theta \in \Theta$, $z_{01}(d) := s_z + \frac{d}{2}\cos\omega$ and $z_{02}(d) := s_z - \frac{d}{2}\cos\omega$. The above result provides an expression to calculate the Fisher information matrix for a general image function and photon detection rate. Hence eq. 3 is applicable to a variety of imaging scenarios including those that give rise to non-radially symmetric image profiles, for example, in the case of imaging single molecules under polarized illumination and/or detection.[10–13] It should be pointed out that the above expression can also be used to determine the 3D resolution measure for any microscopic object (e.g., vesicles, tubules etc.) provided the image function of that object is known.

2.1.1. Special case 1: Point sources lie parallel to the x axis

Previously, we derived an analytical expression of the Fisher information matrix for the resolution problem when the point sources lie in the focal plane of the objective lens and are parallel to the x axis.[5] For the schematic shown in Fig. 1, this pertains to the case when $\omega = \pi/2$ and $\phi = 0$. Substituting this in eq. 3, we have

$$
\mathbf{I}(\theta) := \frac{1}{4} \int_{t_0}^{t} \int_{\mathbb{R}^2} \frac{1}{\Lambda_1(\tau)q_{z_{01}(d),1}(x - \frac{d}{2}, y) + \Lambda_2(\tau)q_{z_{02}(d),2}(x + \frac{d}{2}, y)} \times
$$

$$
\left(\Lambda_1(\tau) \frac{\partial q_{z_{01}(d),1}(x - \frac{d}{2}, y)}{\partial x} - \Lambda_2(\tau) \frac{\partial q_{z_{02}(d),2}(x + \frac{d}{2}, y)}{\partial x} \right)^2 dx\,dy\,d\tau,
$$

(4)

where $\theta \in \Theta$ and $z_{01}(d) = z_{02}(d) = s_z$.

2.1.2. Special case 2: Point sources lie parallel to the z (optical) axis

Consider the scenario where the two point sources lie parallel to the z (optical) axis. For this case, the orientation angle $\omega = 0$. Substituting this in eq. 3, we have

$$
\mathbf{I}(\theta) = \frac{1}{4} \int_{t_0}^{t} \int_{\mathbb{R}^2} \frac{1}{\Lambda_1(\tau)q_{z_{01}(d),1}(x, y) + \Lambda_2(\tau)q_{z_{02}(d),2}(x, y)} \left(\Lambda_1(\tau) \frac{\partial q_{z_{01}(d),1}(x, y)}{\partial z_{01}(d)} - \Lambda_2(\tau) \frac{\partial q_{z_{02}(d),2}(x, y)}{\partial z_{02}(d)} \right)^2 dx\,dy\,d\tau,
$$
(5)

where $\theta \in \Theta$, $z_{01}(d) := s_z + \frac{d}{2}$ and $z_{02}(d) := s_z - \frac{d}{2}$. Suppose, in addition, we assume a very special scenario, where 1.) $s_z = 0$, i.e., the point sources are equidistant from the focal plane with one point source being above the focal plane and the other point source being below the focal plane, 2.) the photon detection rates and the image functions of the two point sources are identical, i.e., $\Lambda_1(\tau) = \Lambda_2(\tau)$, $\tau \geq t_0$, and $q_{z_0,1}(x, y) = q_{z_0,2}(x, y)$ for $(x, y, z_0) \in \mathbb{R}^3$, 3.) the image function $q_{z_0,1}$ is symmetric along the optical axis, i.e., $q_{z_0,1}(x, y) = q_{-z_0,1}(x, y)$, $(x, y) \in \mathbb{R}^2$, $z_0 \in \mathbb{R}$, 4.) the partial derivative of the image function with respect to z_0 is symmetric along the x and y axis with respect to $(x, y) = (0, 0)$, i.e., $\partial q_{z_0,1}(x, y)/\partial z_0 = \partial q_{z_0,1}(-x, y)/\partial z_0 = \partial q_{z_0,1}(x, -y)/\partial z_0$, $(x, y) \in \mathbb{R}^2$, $z_0 \in \mathbb{R}$. Using the above assumptions in eq. 5, it can be shown that the Fisher information matrix is zero. An immediate implication of this result is that for the above imaging conditions, it is not possible to resolve the distance between two point sources if they lie on the optical axis.

2.2. 3D image of a single molecule

In eq. 3, we obtained an expression for the Fisher information matrix for a general image function. In this section we present an analytical expression for the image function of a point source. According to scalar diffraction theory, the image of a self-luminous point source (i.e., fluorescent single molecule) that is located at $(0, 0, z_0)$ in the object space and imaged by a fluorescence microscope can be modeled as[14]

$$I_{z_0}(x, y) = \left| \frac{C}{z_d} \int_0^1 J_0 \left(ka\rho \frac{\sqrt{x^2 + y^2}}{z_d} \right) \exp(jW_{z_0}(\rho))\rho d\rho \right|^2 , \tag{6}$$

where $(x, y) \in \mathbb{R}^2$ denotes an arbitrary point on the detector plane, z_d denotes the axial distance of the detector from the back focal plane of the microscope lens system, C is a constant with complex amplitude, $k = 2\pi/\lambda$, λ denotes the wavelength of the detected photons, a denotes the radius of the limiting aperture of the microscope projected onto the back focal plane of the lens system, J_0 denotes the zeroth order Bessel function of the first kind and $W_{z_0}(\rho)$, $\rho \in [0, 1]$, denotes the phase aberration term. We note that eq. 6 provides a general expression for several 3D point spread function models[14] which describe the image of a point-source/single-molecule and are based on scalar diffraction theory. Rewriting eq. 6 in terms of an image function, we have

$$q_{z_0}(x, y) = \frac{1}{C_{z_0}} \left(U_{z_0}^2(x, y) + V_{z_0}^2(x, y) \right), \quad (x, y) \in \mathbb{R}^2, \quad z_0 \in \mathbb{R}, \tag{7}$$

where

$$U_{z_0}(x, y) := \int_0^1 J_0 \left(ka\rho \frac{\sqrt{x^2 + y^2}}{z_d} \right) \cos(W_{z_0}(\rho))\rho d\rho, \quad (x, y) \in \mathbb{R}^2, \quad z_0 \in \mathbb{R},$$

$$V_{z_0}(x, y) := \int_0^1 J_0 \left(ka\rho \frac{\sqrt{x^2 + y^2}}{z_d} \right) \sin(W_{z_0}(\rho))\rho d\rho, \quad (x, y) \in \mathbb{R}^2, \quad z_0 \in \mathbb{R},$$

$$C_{z_0} = \int_{\mathbb{R}^2} (U_{z_0}^2(x, y) + V_{z_0}^2(x, y)) dxdy, \quad z_0 \in \mathbb{R}. \tag{8}$$

In the above equation U_{z_0} (V_{z_0}) denotes the real (imaginary) part of I_{z_0} given in eq. 6. The term C_{z_0} is the normalization constant, and the $1/C_{z_0}$ scaling in eq. 7 ensures that $\int_{\mathbb{R}^2} f_{\theta_c,\tau}(r) dr = (1/M^2) \int_{\mathbb{R}^2} q_{z_0} \left(\frac{x}{M} - x_0, \frac{y}{M} - y_0 \right) dxdy$ = 1, $\theta_c \in \Theta_c$. Although, not shown explicitly, it can be verified that the partial derivative of the image function q_{z_0} with respect to z_0 is symmetric along the x and y axes with respect to $(x, y) = (0, 0)$.

To calculate the 3D FREM, we require an explicit analytical expression for the phase aberration term W_{z_0} and here, we set W_{z_0} to be

$$W_{z_0}(\rho) := \frac{\pi(n_a)^2 z_0}{n_{med}\lambda} \rho^2, \quad \rho \in [0, 1], \quad z_0 \in \mathbb{R}, \tag{9}$$

where n_a denotes the numerical aperture of the objective lens, n_{med} denotes the refractive index of the medium in the object space and z_0 denotes the axial coordinate of the single molecule in the object space. The above expression for W_{z_0} corresponds to the classical 'Born and Wolf' 3D point spread function model.[15] It can be easily verified that for the above specific expression of W_{z_0}, the image function q_{z_0} is symmetric along the z axis with respect to the point $z = 0$. To calculate the 3D resolution measure, we make use of the expression given by eq. 7 and in eq. 9 we substitute the axial coordinates of the single molecules, which are given $z_{01}(d) = s_z + \frac{d\cos\omega}{2}$ and $z_{02}(d) = s_z - \frac{d\cos\omega}{2}$, where ω denotes the angle subtended by the line segment joining the two single molecules with respect to the z (optical) axis and d denotes the distance of separation between the two single molecules (see Fig. 1).

3. 3D FUNDAMENTAL RESOLUTION MEASURE - 3D FREM

For the derivation of the 3D fundamental resolution measure, we consider two equal intensity single molecules, i.e., $\Lambda_1(\tau) = \Lambda_2(\tau) = \Lambda_0$, $\tau \geq t_0$, where we assume the photon detection rate to be a constant, which is typically assumed in single molecule data analysis.[16, 17] We also assume the image functions of the two single molecules
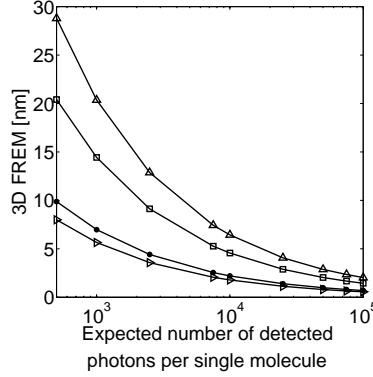
Figure 2. Dependence of the 3D FREM on photon count. The figure shows the 3D FREM as a function of the expected number of detected photons per single molecule for distances of 10 nm ($\triangle$), 20 nm ($\square$), 100 nm ($\bullet$) and 500 nm ($\triangleright$). For all the plots, the numerical aperture is set to be $n_a = 1.3$, the wavelength is set to be $\lambda = 520$ nm, the refractive index of the medium in the object space is set to be $n_{med} = 1.33$, $s_z = 0$ and the orientation angles are set to be $\omega = \pi/4$ and $\phi = 0$.

to be identical, i.e., $q_{z_0,1}(x, y) = q_{z_0,2}(x, y)$, $(x, y) \in \mathbb{R}^2$, $z_0 \in \mathbb{R}$, and that $s_z = 0$, i.e., the single molecules are equidistant from the focal plane of the objective lens such that one single molecule is above the focal plane and the other single molecule is below the focal plane (see Fig. 1). Substituting for q_{z_0} (eq. 7) in the expression for $\mathbf{I}(\theta)$ (eq. 3) and taking the square root of $1/\mathbf{I}(\theta)$, we obtain an analytical expression for the 3D fundamental resolution measure. The 3D FREM predicts how accurately the distance d between two point sources can be resolved. A small numerical value for the 3D FREM predicts high accuracy in determining d, whereas a large numerical value of the 3D FREM predicts low accuracy in determining d. According to the classical axial resolution criteria,[15] two point sources that lie on the optical axis (z axis) are set to be resolved if their distance of separation is greater than or equal to $2\lambda n_{med}/n_a^2$, where λ denotes the wavelength of the detected photons, n_{med} denotes the refractive index of the medium in the object space in which the point sources are present and n_a denotes the numerical aperture of the objective lens. For the GFP molecules, the classical axial resolution criteria predicts the smallest resolvable distance along the optical axis to be 818 nm. The 3D FREM, on the other hand, predicts that distances well below the classical resolution limit can be resolved with relatively high accuracy. For instance, the 3D FREM predicts an accuracy of ±3.58 nm and ±4.41 nm to resolve distances of 500 nm and 100 nm, respectively, between the two single molecules when they lie on the $X - Z$ plane ($\phi = 0$) with $\omega = \pi/4$. For very small distances, however, the 3D FREM predicts poor accuracy in resolving the distance. For example, the 3D FREM predicts an accuracy of ±9.13 nm and ±12.88 nm to resolve distances of 20 nm and 10 nm, respectively. Previously we showed that the fundamental resolution measure FREM, which pertains to the in focus scenario, exhibited an inverse square root dependence on the expected number of detected photons from the single molecules.[5] Analogously, for the 3D case, the resolution measure 3D FREM also exhibits an inverse square root dependence on the expected photon count. This implies that for small distances where the 3D FREM predicts poor accuracy, the resolution measure can be improved by collecting more photons per single molecule (Fig. 2). For example, for a photon count of 2500 photons per single molecule, the 3D FREM predicts an accuracy of ±12.88 nm to resolve a distance of 10 nm when the two single molecules lie in the $X - Z$ plane with $\omega = \pi/4$. If, however, 25000 photons per single molecule are collected then the same distance can be resolved with an accuracy of ±4.07 nm.

4. EFFECTS OF PIXELATION AND NOISE

In deriving the 3D FREM, we assumed that the acquired data was not affected by deteriorating experimental factors such as pixelation of the detector and extraneous noise sources. In this regard, the 3D FREM provides the best case scenario for the achievable resolution measure. In this section, we present results of the 3D resolution measure that take into account deteriorating factors. We refer to this result as the 3D practical resolution measure 3D PREM. The 3D PREM takes into account the presence of additive noise sources, namely Poisson
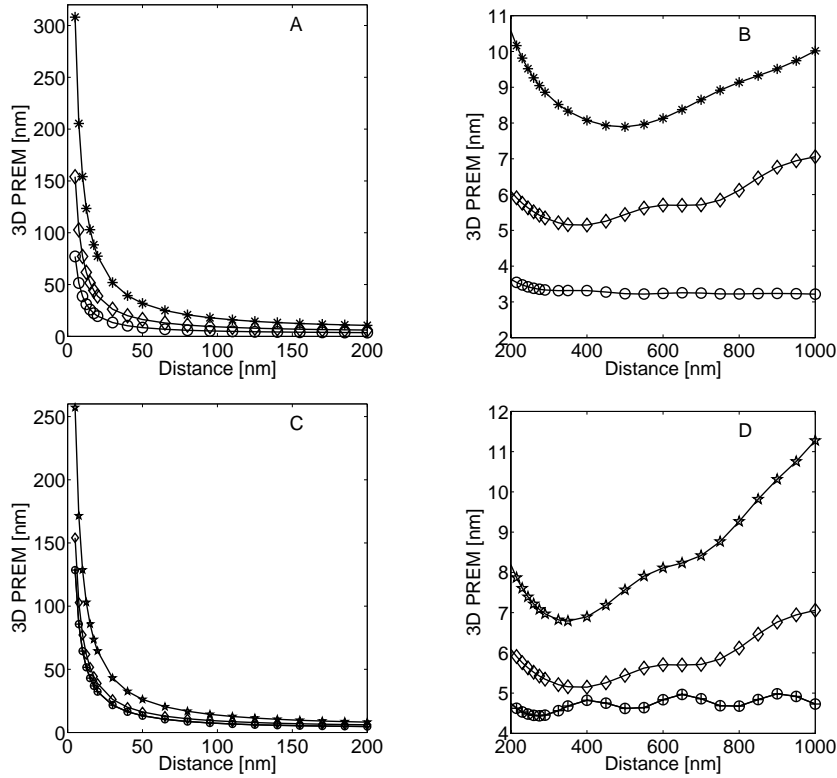
Figure 3. Dependence of the 3D PREM on distance. Panels A and B show the 3D PREM as a function of distance between two GFP single molecules for a pixelated detector in the absence of extraneous noise sources with $\omega = \pi/6$ ($*$) and $\omega = \pi/4$ ($\diamond$). The panels also show the PREM, which corresponds to the in focus scenario ($\omega = \pi/2$), for a pixelated detector in the absence of extraneous noise sources ($\circ$). For all the plots in this panel, the angle ϕ is set to zero. Panels C and D show the 3D PREM as a function of distance for a pixelated detector in the presence ($\star$) and absence ($\diamond$) of extraneous noise sources for $\phi = 0$ and $\omega = \pi/4$. The panels also show the PREM, which corresponds to the in focus scenario, for a pixelated detector in the presence of noise sources ($\oplus$). In all the panels, the pixel size is set to be 13 $\mu m \times 13$ μm, the pixel array size is set to be 21×21, the mean of the additive Poisson noise is set to be 80 photons/pixel/s, the mean and standard deviation of the additive Gaussian noise are set to be 0 e$-$ per pixel and 8 e^- per pixel, respectively, the noise statistics is assumed to be the same for all the pixels and the center of the line segment joining the two single molecules is positioned at the center of the pixel array. The numerical values of all other parameters are identical to those used in Fig. 2.

and Gaussian noise (see Refs. 5, 6, 18 for details). The additive Poisson noise considered here is distinct from the shot noise, which describes the statistics of the photon detection process from the single molecules and is already accounted for by the 3D FREM. Aside from these extraneous noise sources, the PREM also takes into account the effect of pixelation of the detector.

Fig. 3A (3B) shows the behavior of the 3D PREM as a function of the distance between two GFP molecules in the absence of extraneous noise sources for a pixelated detector. Here we assume imaging conditions identical to those assumed in Fig. 2. In particular, the single molecules are assumed to lie on the $X - Z$ plane ($\phi = 0$) and we consider two values of ω, i.e., $\omega = \pi/4$ and $\omega = \pi/6$. Fig. 3A (3B) also shows the 2D PREM for reference, which pertains to the scenario when the single molecules are in focus (i.e., $\omega = \pi/2$). From the figure we see that for a given value of ω, as the distance of separation between the single molecules increases, the numerical value of the 3D PREM first decreases but then gradually increases for very large distances (see Fig. 3B). For small distances of separation, there exists significant uncertainty in resolving the distance between the two single molecules. Hence the 3D PREM exhibits a large numerical value. As the distance of separation increases, the resolvability of the single molecules improves thereby resulting in a smaller numerical value of 3D PREM.

Because the single molecules are out of focus, as the distance of separation increases, less number of photons are collected on the detector, thereby resulting in a deterioration of the 3D PREM for very large distances.

Note that for a given distance of separation, the 3D PREM consistently deteriorates as the orientation angle ω decreases from $\omega = \pi/2$, which corresponds to the in focus scenario, to $\omega = 0$, which corresponds to the scenario when the single molecules are on the optical axis. For instance, for the in focus scenario (i.e., $\omega = \pi/2$), the PREM predicts an accuracy of ± 19.59 nm to resolve a distance of 20 nm. When the single molecules lie on the X-Z plane with $\omega = \pi/4$, the 3D PREM predicts an accuracy of ± 38.86 nm to resolve a distance of 20 nm. On the other hand, if the orientation angle $\omega = \pi/6$, then 3D PREM predicts an accuracy of ± 77.41 nm to resolve the same distance. As discussed in Section 2.1.2, when $\omega = 0$, i.e., when the point sources lie on the optical axis, then the Fisher information matrix becomes zero thereby implying very high uncertainty in determining the distance of separation between the two single molecules.

Fig. 3C (3D) shows the behavior of the 3D PREM as a function of distance for a pixelated detector in the presence and absence of extraneous noise sources. The figure also shows the PREM, which corresponds to the in focus case ($\omega = \pi/2$), for a pixelated detector in the presence of extraneous noise sources. From the figure we see that the numerical value of the 3D PREM in the presence of noise sources is consistently larger than that of the 3D PREM in the absence of noise sources. In particular, for small distances of separation, there is a two fold deterioration in the resolution measure when taking into account noise sources. For instance, in the absence of noise sources, the 3D PREM predicts an accuracy of ± 38.86 nm and ± 77.16 nm to resolve distances of 20 nm and 10 nm, respectively, when the single molecules lie on the $X - Z$ plane with $\omega = \pi/4$. In the presence of noise sources, the 3D PREM predicts an accuracy of ± 64.48 nm and ± 128.5 nm to resolve distances of 20 nm and 10 nm, respectively, for the same conditions. Note that for the range of distances shown in Fig. 3C, the 3D PREM is consistently larger than the PREM, which corresponds to the in focus scenario.

REFERENCES

1. R. J. Ober, C. Martinez, X. Lai, J. Zhou, and E. S. Ward, "Exocytosis of IgG as mediated by the receptor, FcRn: An analysis at the single molecule level," *Proceedings of the National Academy of Sciences USA* **101**(30), pp. 11076–11081, 2004.
2. M. P. Gordon, T. Ha, and P. R. Selvin, "Single molecule high resolution imaging with photobleaching," *Proc. Natl. Acad. Sci. USA* **101**(17), pp. 6462–6465, 2004.
3. X. Qu, D. Wu, L. Mets, and N. F. Scherer, "Nanometer-localized multiple single-molecule fluorescence microscopy," *Proc. Natl. Acad. Sci. USA* **101**(31), pp. 11298–11303, 2004.
4. K. A. Lidke, B. Rieger, T. M. Jovin, and R. Heintzmann, "Superresolution by localization of quantum dots using blinking statistics," *Opt. Exp.* **13**(18), pp. 7052–7062, 2005.
5. S. Ram, E. S. Ward, and R. J. Ober, "Beyond Rayleigh's criterion: A resolution measure with application to single-molecule microscopy," *Proceedings of the National Academy of Sciences* **103**, pp. 4457–4462, 2006.
6. S. Ram, E. S. Ward, and R. J. Ober, "A stochastic analysis of performance limits for optical microscopes," *Multidimensional Systems and Signal Processing* **17**, pp. 27–58, 2006.
7. C. R. Rao, *Linear statistical inference and its applications.*, Wiley, New York, USA., 1965.
8. D. L. Snyder and M. I. Miller, *Random point processes in time and space.*, Springer Verlag, New York, USA, 2nd ed., 1991.
9. S. Ram. PhD thesis, University of Texas at Arlington/University of Texas Southwestern Medical Center at Dallas, in preparation.
10. P. Török, P. Varga, and G. R. Booker, "Electromagnetic diffraction of light focussed through a planar interface between materials of mismatched refractive indices: structure of the electromagnetic field I," *J. Opt. Soc. Am. A* **12**(10), pp. 2136–2144, 1995.
11. P. Török, P. Varga, Z. Laczik, and G. R. Booker, "Electromagnetic diffraction of light focussed through a planar interface between materials of mismatched refractive indices: an integral representation," *J. Opt. Soc. Am. A* **12**(10), pp. 2660–2671, 1995.
12. J. Enderlein, "Theoretical study of detection of a dipole emitter through an objective with high numerical aperture," *Opt. Letts.* **25**(9), pp. 634–636, 2000.

13. M. Böhmer and J. Enderlein, "Orientation imaging of single molecules by wide-field epifluorescence microscopy," *J. Opt. Soc. Am. B* **20**(3), pp. 554–559, 2003.

14. S. F. F. Gibson, *Modeling the 3D imaging properties of the fluorescence light microscope*. PhD thesis, Carnegie-Mellon University, 1990.

15. M. Born and E. Wolf, *Principles of Optics*, Cambridge University Press, Cambridge, UK, 1999.

16. R. E. Thompson, D. R. Larson, and W. W. Webb, "Precise nanometer localization analysis for individual fluorescent probes," *Biophys. J.* **82**, pp. 2775–2783, 2002.

17. U. Kubitscheck, O. Kückmann, T. Kues, and R. Peters, "Imaging and tracking single GFP molecules in solution," *Biophys. J.* **78**, pp. 2170–2179, 2000.

18. R. J. Ober, S. Ram, and E. S. Ward, "Localization accuracy in single molecule microscopy," *Biophys. J.* **86**, pp. 1185–1200, 2004.